msp

Algebraic & Geometric Topology 20 (2020) 343–373

Trisections of surface complements and the Price twist

SEUNGWON KIM
MAGGIE MILLER

Given a real projective plane S embedded in a 4–manifold X^4 with Euler number 2 or -2, the Price twist is a surgery operation on $\nu(S)$ yielding (up to) three different 4–manifolds: X^4, $\tau_S(X^4)$ and $\Sigma_S(X^4)$. This is of particular interest when $X^4 = S^4$, as then $\Sigma_S(X^4)$ is a homotopy 4–sphere which is not obviously diffeomorphic to S^4. Here we show how to produce a trisection description of each Price twist on $S \subset X^4$ by producing a relative trisection of $X^4 \setminus \nu(S)$. Moreover, we show how to produce a trisection description of general surface complements in 4–manifolds.

57M50, 57R65

1 Introduction

In 2012, Gay and Kirby [9] introduced *trisections* of closed 4–manifolds, an analogue of Heegaard splittings of 3–manifolds. During the past six years, topologists have extended this idea to various objects such as 4–manifolds with boundary (see Castro [5]), knotted surfaces in 4–manifolds (see Meier and Zupan [18]), and finitely presented groups (see Abrams, Gay and Kirby [1]). Furthermore, trisections have been used to study classical problems in topology, such as the generalized property R conjecture (some cases were solved by Meier, Schirmer and Zupan [16]) and the Thom conjecture (which was reproved using trisections by Lambert-Cole [14]). Recently, Gay and Meier [10] have studied surgery on spheres in S^4 (including the Gluck twist and blowdown), by constructing trisections of sphere complements in 4–manifolds. Here we study the *Price twist* [20], which is a generalization of the Gluck twist (surgering an $\mathbb{R}P^2$ rather than an S^2), by constructing trisections of general surface complements in 4–manifolds.

This paper is organized as follows. In Section 2, we give definitions of various notions of trisection. In Section 3, we describe the Price twist. In Section 4, we show how to produce a relative trisection of a surface complement in a 4–manifold. Lastly, in Section 5 we give a procedure that produces a trisection of a 4–manifold arising from a Price twist.

Published: 23 February 2020 DOI: 10.2140/agt.2020.20.343

Acknowledgements

Thanks to Jeff Meier, David Gay and Alex Zupan for helpful conversations about surface complements (especially at CIRM 2018 and BIRS–CMO 2017). Thanks to Selman Akbulut for making us aware of plugs in 4–manifolds at the AMS 2018 Spring Eastern Sectional Meeting. Miller also thanks her graduate advisor, David Gabai. Finally, we thank an anonymous referee for thoroughly reading this paper and providing many helpful comments.

Kim is supported by the National Institute for Mathematical Sciences South Korea (NIMS). Miller is a fellow in the National Science Foundation Graduate Research Fellowship program, under Grant No. DGE-1656466.

2 Trisection, relative trisection and bridge trisection

2.1 Definitions

First, we define a trisection of a closed 4–manifold.

Definition 2.1 [9] Let X^4 be a closed 4–manifold. A (g,k)–*trisection* of X^4 is a triple (X_1, X_2, X_3) where

- $X_1 \cup X_2 \cup X_3 = X^4$,
- $X_i \cong \natural_k S^1 \times B^3$,
- $X_i \cap X_j = \partial X_i \cap \partial X_j \cong \natural_g S^1 \times B^2$,
- $X_1 \cap X_2 \cap X_3 \cong \Sigma_g$,

where Σ_g is the closed orientable surface of genus g.

Note that from the definition, $(\Sigma_g, X_i \cap X_j, X_i \cap X_k)$ gives a Heegaard splitting of $\partial X_i \cong \#_k(S^1 \times S^2)$. By Laudenbach and Poénaru [15], X^4 is specified by its *spine*, $(\Sigma_g \times D^2) \cup_{i,j} (X_i \cap X_j)$. Therefore, we usually describe a trisection (X_1, X_2, X_3) by a *trisection diagram* $(\Sigma_g, \alpha, \beta, \gamma)$ where each of α, β and γ consists of g independent curves bounding disks in the handlebodies $X_1 \cap X_2$, $X_2 \cap X_3$ and $X_1 \cap X_3$, respectively. We generally depict this diagram by drawing on Σ_g the α curves in red, the β curves in blue and the γ curves in green. One typically uses the names $H_\alpha := X_1 \cap X_2$, $H_\beta := X_2 \cap X_3$ and $H_\gamma := X_3 \cap X_1$ for the double intersections. In words, H_α is usually called "the α handlebody" (and similarly H_β is the β handlebody and H_γ is the γ handlebody).

For expositions of trisections, refer to [9] or [16].

Next, we define a relative trisection of a compact 4–manifold with boundary.

Definition 2.2 [9] Let X^4 be a compact 4–manifold with boundary $M^3 \neq \varnothing$. A (g,k,p,b)–*relative trisection* of X^4 is a triple (X_1, X_2, X_3) where

- $X_1 \cup X_2 \cup X_3 = X^4$,
- $X_i \cong \natural_k S^1 \times B^3$,
- $X_i \cap X_j = \partial X_i \cap \partial X_j \cong (\Sigma_g^b \times I) \cup (g-p \text{ 2–handles}) \cong \natural_{g+b+p-1} S^1 \times B^2$,
- $X_1 \cap X_2 \cap X_3 \cong \Sigma_g^b$,

where Σ_g^b is an orientable surface of genus g and $b > 0$ boundary components. In $X_i \cap X_j$, the $g-p$ 2–handles are attached to cancel $g-p$ 1–handles of $\Sigma_g^b \times I$. This ensures $X_i \cap X_j$ is a 3–dimensional handlebody of genus $g+p+b-1$. Moreover, we have the following conditions on M^3:

- $X_i \cap X_j \cap M^3 \cong \Sigma_p^b$,
- $X_i \cap M^3 = (X_i \cap X_j \cap M^3) \times I$.

Thus, (X_1, X_2, X_3) determines an open book decomposition on M^3, where each $X_i \cap X_j \cap M^3$ is a single page. (In particular, if M is connected, then $X_i \cap X_j \cap M^3$ must be connected.)

Relative trisections of X^4 and Y^4 with $\partial X^4 \cong \partial Y^4$ can be glued to form a trisection of $X^4 \cup_\partial Y^4$ if and only if the relative trisections induce the same (isotopic) open books on $\partial X^4 \cong \partial Y^4$, but with opposite orientations [5].

Again, X^4 is specified by its *spine*, $(\Sigma_g^b \times D^2) \cup_{i,j} (X_i \cap X_j)$ [6]. Therefore, we usually describe a relative trisection (X_1, X_2, X_3) by a *relative trisection diagram* $(\Sigma_g^b, \alpha, \beta, \gamma)$ where each of α, β and γ consists of $g-p$ independent curves bounding disks in the compression bodies $X_1 \cap X_2$, $X_2 \cap X_3$ and $X_1 \cap X_3$, respectively, with notation for the intersections and conventions as above.

For expositions of relative trisections, refer to [5], [6] or [8].

Lastly, we define a bridge trisection of a knotted surface in an arbitrary 4–manifold.

Definition 2.3 Let S be a surface embedded in a 4–manifold X^4. Say X^4 has a (g,k)–trisection (X_1, X_2, X_3). By [18], S can be isotoped so that

- $S \cap X_i$ is a disjoint union of c–boundary parallel disks,
- $S \cap X_i \cap X_j$ is a trivial tangle of b arcs.

Note $\chi(S) = 3c - b$. We say S is in (c,b)–*bridge position* in X^4 with respect to (X_1, X_2, X_3), or that (X_1, X_2, X_3) induces a (c,b)–*bridge trisection* on S. We can stabilize (X_1, X_2, X_3) to find a trisection $(\widetilde{X}_1, \widetilde{X}_2, \widetilde{X}_3)$ which induces a $(1, b-3(c-1))$–bridge trisection on S [18].

For expositions on bridge trisections of surfaces in 4–manifolds, see [17] or [18].

Bridge trisections admit two kinds of diagrams. One is a diagram (in the standard sense) of the triple of tangles $(X_i \cap X_{i+1}, S \cap X_i \cap X_{i+1})|_{i=1,2,3}$ (where $X_4 := X_1$). When $g = 0$, this diagram consists of 3–tangle diagrams in disks. This is usually called a *triplane diagram*. Another kind of diagram is the *shadow diagram*. The shadow diagram is less likely to be familiar to the average reader, so we expand more upon its definition.

Definition 2.4 Let S be a surface in (c,b)–bridge position in X^4 with respect to the (g,k)–trisection (X_1, X_2, X_3). Let $(\Sigma_g, \alpha, \beta, \gamma)$ be a trisection diagram of (X_1, X_2, X_3). Identify Σ_g with $X_1 \cap X_2 \cap X_3$. A *shadow diagram* for S is a septuple of the form $(\Sigma_g, \alpha, \beta, \gamma, s_\alpha, s_\beta, s_\gamma)$ where:

- Each s_* is a collection of b disjoint arcs in Σ_g with $\partial s_* = S \cap \Sigma_g$.
- The collection of c circles $(S \cap (X_1 \cap X_2)) \cup s_\alpha$ bounds a set of c disjoint embedded disks D_α in $X_1 \cap X_2$, with $\mathring{D}_\alpha \cap (\partial(X_1 \cap X_2)) = \varnothing$. That is, s_α can be obtained by projecting the boundary-parallel tangle $S \cap (X_1 \cap X_2)$ onto $\partial(X_1 \cap X_2) = \Sigma$.
- Similarly, s_β and s_γ can be obtained by projecting the boundary-parallel tangles $S \cap (X_2 \cap X_3) \subset X_2 \cap X_3$ and $S \cap (X_1 \cap X_3) \subset X_1 \cap X_3$ onto Σ_g, respectively.

In this paper, whenever we draw a shadow diagram $(\Sigma_g, \alpha, \beta, \gamma, s_\alpha, s_\beta, s_\gamma)$, we will draw the curves α, β and γ and arcs s_α, s_β and s_γ on the surface Σ. The α curves and s_α arcs will be red; the β curves and s_β arcs will be blue; the γ curves and s_γ arcs will be green. The endpoints of s_* will be indicated with black dots. See Figure 1 for a small example of a shadow diagram.

The shadow diagram $(\Sigma_g, \alpha, \beta, \gamma, s_\alpha, s_\beta, s_\gamma)$ determines each $X_i \cap X_j$ (up to diffeomorphism) and $S \cap (X_i \cap X_j)$ (up to isotopy). Since $S \cap X_i$ consists of boundary-parallel disks, this determines S up to isotopy.

See [17; 18] for the original definitions of triplane and shadow diagrams and many examples.

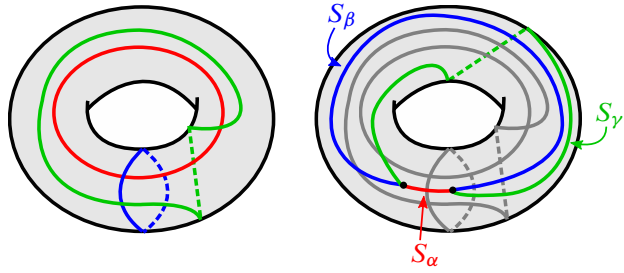

Figure 1: A trisection diagram $(\Sigma_1, \alpha, \beta, \gamma)$ for $\mathbb{C}P^2$ (left) and a shadow diagram $(\Sigma_1, \alpha, \beta, \gamma, s_\alpha, s_\beta, s_\gamma)$ for a surface in $\mathbb{C}P^2$ (right). The α, β and γ curves are visible in the left diagram, so we dim them on the right to make the shadow arcs s_* more visible. The described surface is in $(1,1)$–bridge position, so the surface is a sphere. (In fact, this is a shadow diagram for the standard $\mathbb{C}P^1$.)

2.2 Kirby diagrams from relative trisections

In this subsection, we discuss how to obtain a Kirby diagram of X^4 from a relative trisection of X^4. This essentially comes from Lemma 14 of [9] (although they only consider closed manifolds, the procedure is almost exactly the same for manifolds with boundary). An alternative viewpoint is found in [16].

Let $(\Sigma, \alpha, \beta, \gamma)$ be a (g,k,p,b)–relative trisection of X^4. Consider the following handle structure on X^4:

- One 0–handle and k 1–handles, glued to make X_1.
- $g-k+p+b-1$ 2–handles, corresponding to γ curves which are dual to the β curves (up to handle-slides). These handles are glued to the 0– and 1–handles so that $X_2 = (H_\beta \times I) \cup (\text{2–handles})$.
- $k-2p-b+1$ 3–handles, corresponding to parallel (up to handle-slides) α and γ curves. Then $X_3 = ((H_\alpha \cup_\Sigma H_\gamma) \times I) \cup (\text{3–handles})$.

In practice, drawing the Kirby diagram for this handle decomposition is simple when there are no 3–handles (ie $k-2p-b+1=0$, ie there are no parallel α and γ curves). Perform handle-slides on the α and β curves so that the pair (α, β) is standard. Then draw a 1–handle for each cut arc in the α and β pages and for each parallel α and β curve; draw a 2–handle for each γ curve with framing given by the surface framing. See Figure 2.

In the above procedure, the 2–handles, 3–handles, and the 1–handles corresponding to parallel α and β curves should be familiar to a reader who has seen the construction

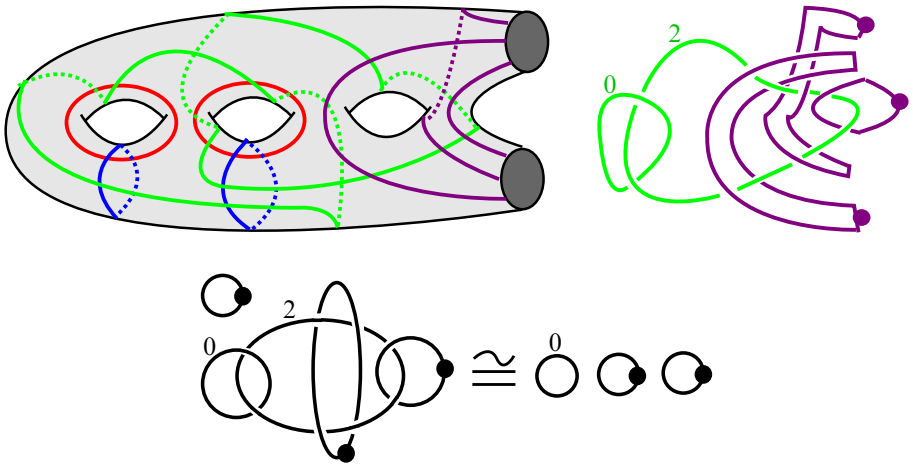

Figure 2: Top left: A $(g,k,p,b)=(3,3,1,2)$–trisection diagram. Here, α and β are standard. We have drawn a cut-system (purple) for the α and β pages. Top right: We find a Kirby diagram for the pictured 4–manifold. Each cut arc doubles to a 1–handle curve; push one copy into the α compression body ("outside the surface") and the other into the β–compression body ("inside the surface"). The γ curves become 2–handle attaching circles with framing given by the surface framing. There are no 3– or 4–handles. Bottom: We can now easily see that the pictured 4–manifold is $(S^2\times D^2)\natural(S^1\times B^3)\natural(S^1\times B^3)$.

of a Kirby diagram for a closed 4–manifold from a trisection [9]. The 1–handles corresponding to cut arcs are more novel. These are apparent by actually considering the gluing $H_\alpha\cup_\Sigma H_\beta$. Take $H_\beta=\Sigma\times[0,1]\cup(\text{2–handles along }\beta\times 0)$ to be the standard compression body in S^3 (see Figure 3). For each α curve dual to a β curve, a 2–handle can be glued to $\alpha\times 1$ in S^3. For each α curve parallel to a β curve, we add

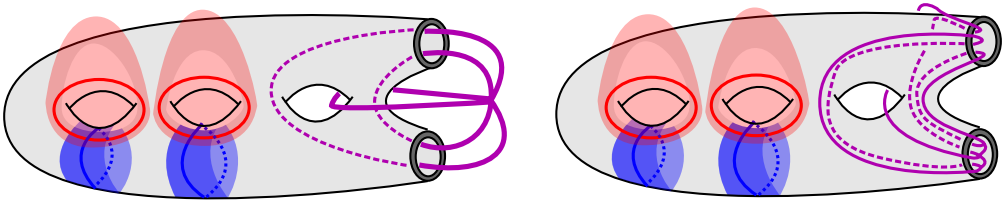

Figure 3: We still consider the relative trisection of Figure 2. Left: $H_\alpha\cup_\Sigma H_\beta$ lies inside $\#_{k-2p-b+1}\,S^1\times S^2$. The complement of $H_\alpha\cup_\Sigma H_\beta$ is a handlebody; we have drawn the spine. Right: We isotope the spine to see cores of the handlebody $\left(\#_{k-2p-b+1}\,S^1\times S^2\right)\setminus(H_\alpha\cup_\Sigma H_\beta)$ as doubles of a cut system of the α and β pages.

a parallel dotted circle and attach a 2–handle along $(\alpha \times 1)$ in $\#_{k-2p-b+1}\, S^1 \times S^2$. This yields $H_\alpha \cup_\Sigma H_\beta \subset \#_{k-2p-b+1}\, S^1 \times S^2$.

The boundary of $H_\alpha \cup_\Sigma H_\beta$ consists of the α and β pages glued together along collars of their boundary, so $\partial(H_\alpha \cup_\Sigma H_\beta)$ is a surface of genus $2p+b-1$. Moreover, $\left(\#_{k+2p+b-1}\, S^1 \times S^2\right) \setminus (H_\alpha \cup_\Sigma H_\beta)$ is a handlebody of genus $2p+b-1$. The dotted circles obtained from the cut arcs of the α and β pages are cores of this handlebody (see Figure 3). Add these dotted circles to the diagram so that now $H_\alpha \cup_\Sigma H_\beta$ is embedded in $\#_k\, S^1 \times S^2$, so that $\left(\#_k\, S^1 \times S^2\right) \setminus (H_\alpha \cup_\Sigma H_\beta)$ is a product from the α page to the β page. The total $\#_k\, S^1 \times S^2$ is then exactly ∂X_1.

We take X_2 to be the trace of a cobordism from H_β to H_γ; thicken the β compression body and glue 2–handles for each γ curve that is dual to the β curves (up to handle-slides). By adding 2–handle attaching circles parallel to these γ curves (with framing equal to the surface framing), we can view X_1 and X_2 as living in the 4–manifold described by this Kirby diagram. Finally, to include X_3 in this diagram we attach 3–handles along essential spheres in $H_\alpha \cup_\Sigma H_\gamma$ (ie one 3–handle for each γ curve parallel to an α curve, up to handle-slides.)

Finding a relative trisection of X^4 from a Kirby diagram is more challenging. In [7] Castro, Gay and Pinzón-Caicedo describe how to obtain a relative trisection from a Kirby diagram of X^4 and a page of an open book on ∂X^4 within the diagram.

3 The Price twist

3.1 Introduction

Let S be a real projective plane embedded in a 4–manifold X^4, with Euler number $e(S) = \pm 2$ (eg any $\mathbb{R}P^2$ in S^4). A tubular neighborhood of S admits a handle structure consisting of a 0–handle, a 1–handle, and a 0–framed 2–handle running twice over the 1–handle (Figure 4). We call this tubular neighborhood P_+ or P_-, depending on the sign of $e(S)$. The boundary of P is the quaternion space Q, named because it is the quotient of S^3 by the action of the quaternion group. A perhaps more useful description for low-dimensional topologists is that Q is a Seifert-fibered space over S^2, with three exceptional fibers of index ± 2, ± 2 and ∓ 2. Following [13], we call these fibers S_0, S_1 and S_{-1}. We do not specify the indices of these fibers, as they may be permuted by a homeomorphism of Q. See Figure 4 for an illustration of S_0, S_1 and S_{-1} in $Q = \partial P_-$.

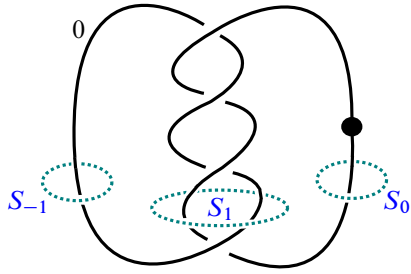

Figure 4: A Kirby diagram of P_-. (Mirror the diagram to obtain P_+.) $Q = \partial P_\pm$ is a Seifert fibered space with three singular fibers S_0, S_1 and S_{-1} as pictured. The S_{-1} fiber bounds a disk in $P_\pm$.

Note $\partial(X^4 \setminus \nu(S)) \cong Q$. Label the singular fibers in $\partial(X^4 \setminus \nu(S))$ so that the trivial regluing of $\nu(S)$ to obtain X^4 corresponds to the map $\partial(\nu(S)) \to \partial(X^4 \setminus S)$ given by $(S_1, S_0, S_{-1}) \mapsto (S_1, S_0, S_{-1})$

Price [20] has classified the self-homeomorphisms of Q, finding that there are six up to isotopy. These maps preserve the Seifert fiber structure, and are determined simply by the induced permutation of the singular fibers. Moreover, Price showed that the map that permutes S_0 and S_1 extends over $P_\pm$. Therefore, there are at most three 4–manifolds (up to diffeomorphism) that may arise from deleting $\nu(S)$ from X^4 and regluing according to ϕ: $\partial\nu(S) \to \partial(X^4 \setminus \nu(S))$. These 4–manifolds are:

- X^4 when $\phi(S_{-1}) = S_{-1}$.
- $\tau_S(X^4)$ when $\phi(S_{-1}) = S_0$. Using the Mayer–Vietoris sequence, we see $H_1(\tau_S(X^4)) \neq H_1(X^4)$.
- $\Sigma_S(X^4)$ when $\phi(S_{-1}) = S_1$.

We call $\Sigma_S(X^4)$ the Price twist of X^4 along S. In the notation of Akbulut and Yasui [4], this operation is equivalent to a certain plug twist. See [4; 3] for more on this point of view. For our purposes, it is enough to notice that the Price twist is a way of constructing potentially exotic 4–manifolds, and is most interesting in the case $X^4 = S^4$. When $X^4 = S^4$, $\Sigma_S(S^4)$ is a homotopy 4–sphere. It is unknown under which conditions $\Sigma_S(X^4)$ is diffeomorphic to X^4. Katanaga et al [13] showed that this operation generalizes the Gluck twist: if K is a 2–sphere smoothly embedded in X^4 with trivial normal bundle, and P is a unknotted real projective plane in a 4–ball disjoint from K, then the Gluck twist of X^4 along K is diffeomorphic to $\Sigma_{K\#P}(X^4)$. In particular, this means that in some cases $\Sigma_S(X^4) \ncong X^4$ (see for example [2]), but there are of course no known examples of this phenomenon in S^4. (In fact, the

authors are unaware of any examples of this phenomenon in any orientable 4–manifold. The surgeries displayed in [2] which change the smooth structure of the ambient 4–manifold all take place in nonorientable 4–manifolds.) Whether the Price twist strictly generalizes the Gluck twist in S^4 is related to the *Kinoshita conjecture*.

Question 3.1 (Kinoshita) Given a real projective plane S smoothly embedded in S^4, can S be decomposed as $K\#P$ for some 2–sphere K and an unknotted real projective plane P?

The answer to the above question is known to be "yes" in some cases; see eg [11]. One might study the Kinoshita conjecture by understanding the basic algebraic topology of $S^4\setminus\nu(S)$. Suppose $S=K\#P$ for a 2–knot K and unknotted real projective plane P. Then $S^4\setminus\nu(S)\cong(S^4\setminus\nu(K))\natural(S^4\setminus\nu(P))$, so $\pi_1(S^4\setminus\nu(S))\cong\pi_1(S^4\setminus K\,|\,[\gamma]^2=0)$, where $[\gamma]$ is a normal generator of $\pi_1(S^4\setminus K)$. Fundamental groups of 2–knot complements have been classified as admitting certain presentations by Kamada [12], so $\pi_1(S^4\setminus\nu(S))\cong\pi_1(\tau_S(S^4))$ is a potential obstruction to S admitting the decomposition $K\#P$.

3.2 Two preferred trisections of $P_{\pm}$

In this section, we describe two particular $(g,k,p,b)=(2,2,0,3)$–relative trisections of P_+ (the mirror images of which are naturally trisections of P_-), shown in Figure 5. Call these trisections T_1 and T_2. From T_i, the discussion in Section 2.2 yields a Kirby diagram, from which we can check that the trisected manifold is indeed P_+

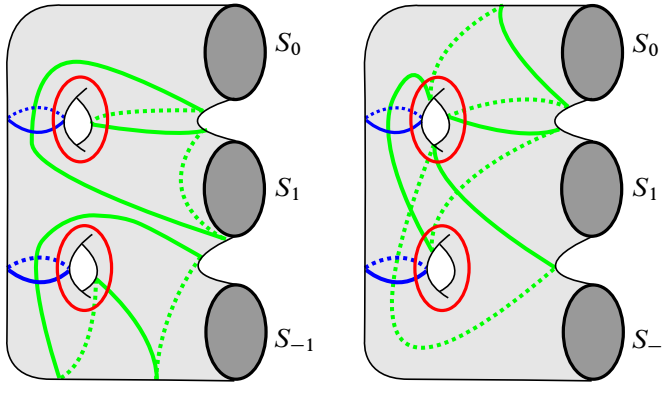

Figure 5: The relative trisections T_1 of P_+ (left) and T_2 of P_+ (right). These are both $(g,k,p,b)=(2,2,0,3)$–relative trisections.

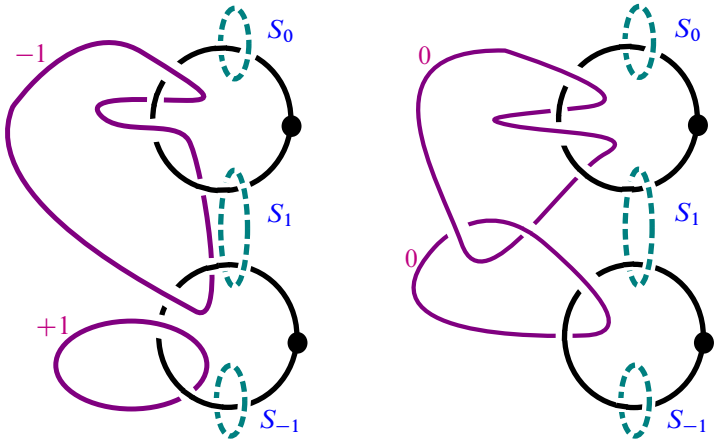

Figure 6: Kirby diagrams obtained from T_1 (left) and T_2 (right). Neither diagram has any 3– or 4–handles. Both depict P_+. The S_i are the bindings of the open book on Q (shown here after some handle-slides).

(see Figure 6). The three singular fibers of $Q = \partial P_+$ form the bindings of the open book induced by T_i on $Q = \partial P_+$, and each page has monodromy consisting of two right-handed Dehn twists around two boundary components and two left-handed Dehn twists around the third. In T_1, the twists around the S_{-1} boundary are left-handed. In T_2, the twists around the S_{-1} boundary are right-handed (see Figures 7 and 8).

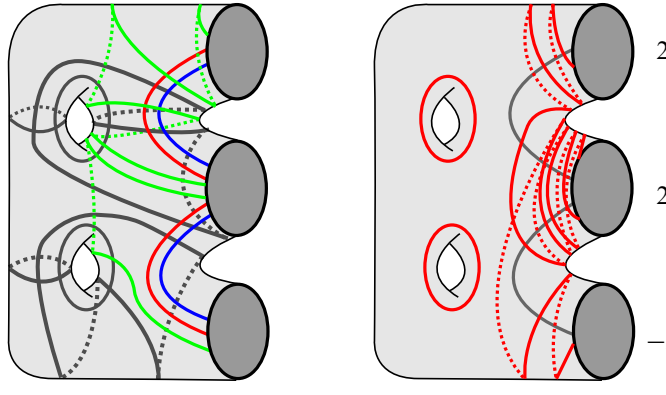

Figure 7: We perform the algorithm of [6] to find the monodromy of the open book induced on Q by T_1. Left: resulting cut systems for each page $X_i \cap X_j \cap \partial P_+$. Right: the effect of the monodromy on the $X_1 \cap X_2 \cap \partial P_+$ system. The monodromy automorphism consists of two right-handed Dehn twists around each of S_0 and S_1 and two left-handed twists around S_{-1}.

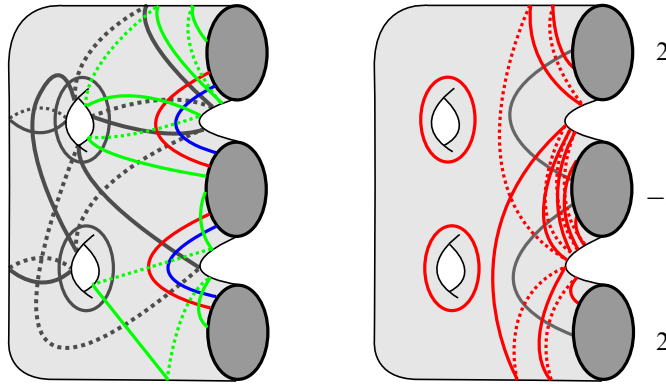

Figure 8: We perform the algorithm of [6] to find the monodromy of the open book induced on Q by T_2. Left: resulting cut systems for each page $X_i \cap X_j \cap \partial P_-$. Right: the effect of the monodromy on the $X_1 \cap X_2 \cap \partial P_+$ system. The monodromy automorphism consists of two right-handed Dehn twists around each of S_0 and S_{-1} and two left-handed twists around S_1.

4 Relative trisections of surface complements

In this section, we show how to produce a relative trisection of the complement of a surface S in a 4–manifold X^4. In particular, we can produce a $(g,k,p,b)=(g,k,0,3)$–trisection of any $\mathbb{R}P^2$ complement in X^4. For notational ease, we will often use the shorthand "$\cap\,\partial$" to denote "$\cap\,\partial(X^4 \setminus \nu(S))$".

Naively, one might attempt to construct a trisection of a surface complement in the following (generally incorrect) way:

- Say X^4 is a 4–manifold with trisection (X_1, X_2, X_3).
- Let $S \subset X^4$ be a surface in (c,b)–bridge position with respect to the trisection (X_1, X_2, X_3).
- Delete a tubular neighborhood of S from each X_i to find a trisection on $X^4 \setminus \nu(S)$.

This procedure is successful exactly when $S \cong S^2$ and $c = 1$ (as in [10]). Otherwise, this procedure *does not* yield a relative trisection of $X^4 \setminus \nu(S)$ for (in part) the following reason. Recall from Definition 2.2 that a relative trisection must induce an open book on the 3–dimensional boundary, with pages $X_i \cap X_j \cap \partial$. In this setting, $((X_i \cap X_j) \setminus \nu(S)) \cap \partial(X^4 \setminus \nu(S)) \cong \bigsqcup_b (S^1 \times I)$, which is a collection of b annuli corresponding to the bridges of S in $X_i \cap X_j$. Note that if $b = 1$, then S is a sphere, since $\chi(S) = 3c - b$. If $b > 1$, then $((X_i \cap X_j) \setminus \nu(S)) \cap \partial(X^4 \setminus \nu(S))$ is disconnected, and certainly cannot be a page in an open book on $\partial(X^4 \setminus (S))$.

To deal with this problem, we introduce an operation on manifolds Y^4 divided into three pieces $Y^4 = Y_1 \cup Y_2 \cup Y_3$ (not necessarily as a relative trisection, but still assuming $Y_i \cap Y_j = \partial Y_i \cap \partial Y_j$) that can reduce the number of components of $Y_i \cap Y_j \cap \partial Y^4$.

Definition 4.1 Let Y^4 be a 4–manifold with nonempty boundary. Write $Y^4 = Y_1 \cup Y_2 \cup Y_3$, where $Y_i \cap Y_j = \partial Y_i \cap \partial Y_j$. Let C be an arc properly embedded in $Y_i \cap Y_j \cap \partial Y^4$ with endpoints in $Y_1 \cap Y_2 \cap Y_3$. Let $\nu(C)$ be a fixed open tubular neighborhood of C. Let

- $\widetilde{Y}_i := Y_i \setminus \nu(C)$,
- $\widetilde{Y}_j := Y_j \setminus \nu(C)$,
- $\widetilde{Y}_k := Y_k \cup \overline{\nu(C)}$.

We refer to the replacement of the triple (Y_1, Y_2, Y_3) by $(\widetilde{Y}_1, \widetilde{Y}_2, \widetilde{Y}_3)$ as a *boundary-stabilization*. We say that we have boundary-stabilized Y_k.

This move is depicted in Figure 11.

We illustrate the effect of this stabilization on each of Y_1, Y_2 and Y_3, double intersection, and triple intersection by studying trisections of $\mathbb{R}P^2$ complements in the following subsection. In Section 4.2, we will use the same principle to trisect the complement of an arbitrary surface complement.

4.1 Trisecting complements of embedded $\mathbb{R}P^2$s

Let (X_1, X_2, X_3) be a (g,k)–trisection of X^4. Let S be an embedded $\mathbb{R}P^2$ in X. By [18], S can be isotoped to be in bridge position with respect to (X_1, X_2, X_3). We stabilize the trisection as in [18] so that $S \cap X_i = D^2$ for each i. Then $S \cap X_i \cap X_j$ is a trivial 2–bridge tangle.

Delete a tubular neighborhood of S from X^4; let $X_i' := X_i \setminus \nu(S)$. For each $i = 1, 2, 3$, with $\{i, j, k\} = \{1, 2, 3\}$, let C_i be an arc in $X_j' \cap X_k' \cap \partial(X^4 \setminus \nu(S))$ (with endpoints in $X_1' \cap X_2' \cap X_3'$) which meets two different boundary components of $X_1' \cap X_2' \cap X_3'$. Take C_1, C_2 and C_3 to have disjoint endpoints, and to twist zero times around the 3–dimensional tubes of $\nu(S) \cap (X_i \cap X_j)$ (ie we ask that $S \cap (X_i \cap X_j)$ cobounds disks D in $X_i \cap X_j$ with arcs in $X_i \cap X_j \cap X_k$ such that $C_k \cap D = \varnothing$). This will not matter until we attempt to find the resulting relative trisection diagram. In principle, one could allow C_i to twist around $\nu(S) \cap (X_j \cap X_k)$ arbitrarily and modify the

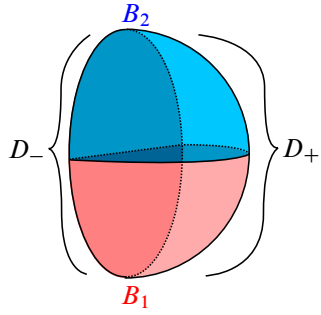

Figure 9: To understand the effect of boundary-stabilizing along arc C in $X_1' \cap X_2' \cap \partial$, we write $\overline{\nu(C)}$ as $[-\epsilon, 1+\epsilon] \times B$, where B is a closed half 3–ball. Here, we draw B. We decompose B into two quarter-balls B_1 and B_2, so that $\overline{\nu(C)} \cap X_1' = I \times B_1$ and $\overline{\nu(C)} \cap X_2' = I \times B_2$. The boundary of B is decomposed into two disks, D_- and D_+ (which both meet B_1 and B_2), so that $\overline{\nu(C)} \cap \partial = [-\epsilon, 1+\epsilon] \times D_-$.

relative trisection accordingly, but for simplicity we restrict the intersection. We will boundary-stabilize each X_i along C_i to find a relative trisection of $X^4 \setminus \nu(S)$.

The boundary-stabilization move of X_3' along $C := C_3$ is pictured in Figures 10 and 11. For ease of discussion, we write $\overline{\nu(C)} = [-\epsilon, 1+\epsilon] \times B$, where B is a (closed) half 3–ball. Write $\partial B = D_+ \cup D_-$, where D_+ and D_- are each disks, and $\nu(C) \cap \partial(X^4 \setminus \nu(S)) = [-\epsilon, 1+\epsilon] \times D_-$. Write B as the union of two quarter (closed) 3–balls B_1 and B_2 along a disk so that $\overline{\nu(C)} \cap X_1' = I \times B_1$, $\overline{\nu(C)} \cap X_2' = I \times B_2$ and $\overline{\nu(C)} \cap X_3' = ([-\epsilon, 0] \cup [1, 1+\epsilon]) \times B$. See Figure 9.

This boundary-stabilization increases the genus of X_3', $X_1' \cap X_3'$ and $X_2' \cap X_3'$ each by one. We illustrate the effect on $X_i' \cap X_j' \cap \partial(X^4 \setminus \nu(S))$ and $X_1' \cap X_2' \cap X_3'$ in Figures 12 and 13; each of these figures relate to a schematic triplane diagram. We discuss the topology of each trisection piece before and after the boundary-stabilization move in greater detail in the following paragraphs. (Many of these paragraphs are repetitive due to the symmetry of a trisection, but we consider each piece separately for clarity.) Recall the notation "$\cap\, \partial$" means "$\cap\, \partial(X^4 \setminus \nu(S))$".

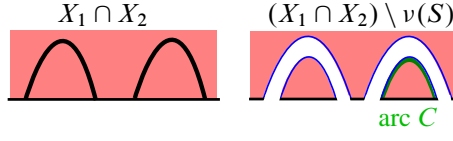

Figure 10: Left: $S \cap X_1 \cap X_2$. Right: we find an arc C in $X_1' \cap X_2' \cap \partial$ which meets two different boundary components of $X_1' \cap X_2' \cap X_3'$ (ie an arc that runs along one bridge).

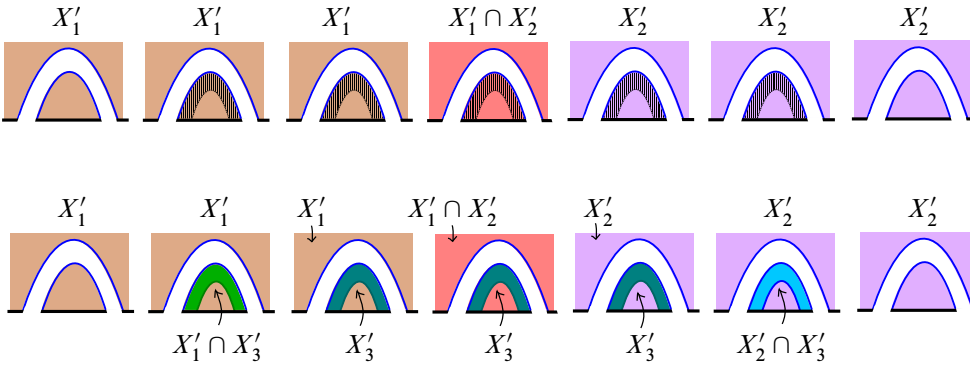

Figure 11: Top: the shaded regions are slices of a neighborhood of C in $X^4 \setminus \nu(S)$ before stabilizing. Bottom: to boundary-stabilize, we declare this neighborhood is in X_3'.

X_1' Before boundary-stabilizing X_3', $X_1' \cong \natural_{k+1} S^1 \times B^3$. After boundary-stabilizing X_3', $X_1' \cong \natural_{k+1} S^1 \times B^3$. From X_1', in the boundary-stabilization we carve out a neighborhood of the arc C in $\partial X_1'$. This does not change the topology of X_1'.

X_2' Before boundary-stabilizing X_3', $X_2' \cong \natural_{k+1} S^1 \times B^3$. After boundary-stabilizing X_3', $X_2' \cong \natural_{k+1} S^1 \times B^3$. From X_2', in the boundary-stabilization we carve out a neighborhood of arc C in $\partial X_2'$. This does not change the topology of X_2'.

X_3' Before boundary-stabilizing X_3', $X_1' \cong \natural_{k+1} S^1 \times B^3$. After boundary-stabilizing X_3', $X_3' \cong \natural_{k+2} S^1 \times B^3$. To X_3', we add a neighborhood of arc C (recall $\partial C \in \partial X_3'$ and $\mathring{C} \cap X_3' = \varnothing$). The effect is to add another boundary-sum $S^1 \times B^3$ component to X_3'.

$X_1' \cap X_2'$ Before boundary-stabilizing X_3', $X_1' \cap X_2' \cong \natural_{g+2} S^1 \times B^2$. After boundary-stabilizing X_3', $X_1' \cap X_2' \cong \natural_{g+2} S^1 \times B^2$. From $X_1' \cap X_2'$, in the boundary-stabilization we carve out a neighborhood of arc C in $\partial X_1' \cap X_2'$. This does not change the topology of $X_1' \cap X_2'$.

$X_2' \cap X_3'$ Before boundary-stabilizing X_3', $X_2' \cap X_3' \cong \natural_{g+2} S^1 \times B^2$. After boundary-stabilizing X_3', $X_2' \cap X_3' \cong \natural_{g+3} S^1 \times B^2$. Then, to $X_2' \cap X_3'$, in the boundary-stabilization we add $I \times B_2$. The effect is to add another boundary-sum $S^1 \times B^2$ component to $X_2' \cap X_3'$.

$X_1' \cap X_3'$ Before boundary-stabilizing X_3', $X_1' \cap X_3' \cong \natural_{g+2} S^1 \times B^2$. After boundary-stabilizing X_3', $X_1' \cap X_3' \cong \natural_{g+3} S^1 \times B^2$. To $X_1' \cap X_3'$, in the boundary-stabilization we add $I \times B_1$. The effect is to add another boundary-sum $S^1 \times B^2$ component to $X_1' \cap X_3'$.

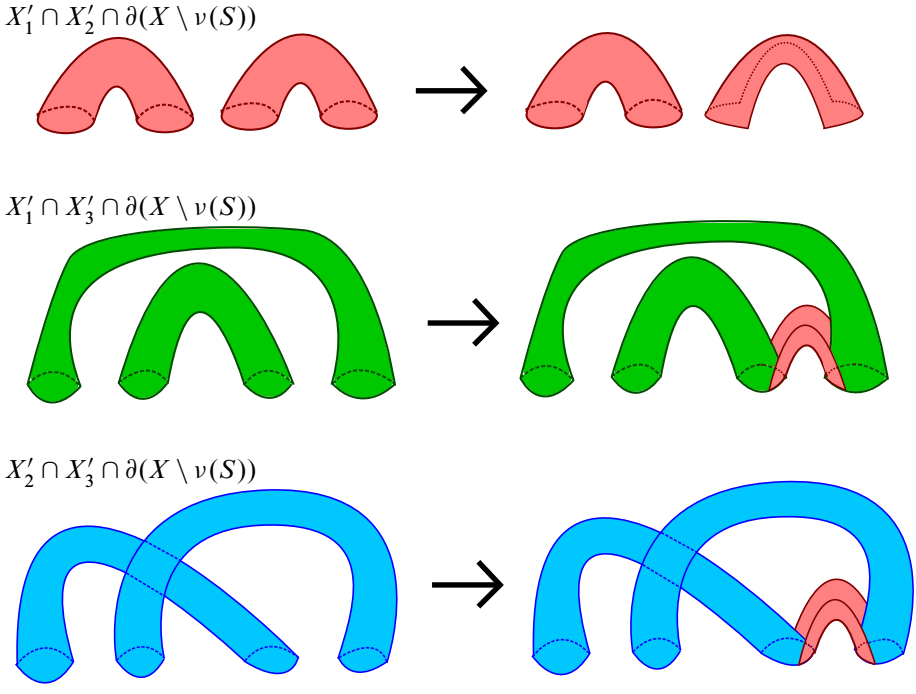

Figure 12: The boundary-stabilization move deletes a band from $X_1' \cap X_2' \cap \partial(X^4 \setminus \nu(S))$, and adds a band to each of $X_1' \cap X_3' \cap \partial$ and $X_2' \cap X_3' \cap \partial$. These are not literally three instances of the same band. The band deleted from $X_1' \cap X_2' \cap \partial$ is $I \times (B_1 \cap B_2 \cap D_-)$. The band added to $X_1' \cap X_3' \cap \partial$ is $I \times (B_1 \cap D_+ \cap D_-)$. The band added to $X_2' \cap X_3'$ is $I \times (B_2 \cap D_+ \cap D_-)$.

$X_1' \cap X_2' \cap X_3'$ Before boundary-stabilizing X_3', $X_1' \cap X_2' \cap X_3' \cong \Sigma_{g,4}$, a genus-$g$ surface with 4 open disks deleted. After boundary-stabilizing X_3', $X_1' \cap X_2' \cap X_3' \cong \Sigma_{g,4} \cup (\text{a band})$. To $X_1' \cap X_2' \cap X_3'$, we add the band $I \times (B_1 \cap B_2 \cap D_+)$. In this case, we have assumed that the band meets two distinct boundary components of $\Sigma_{g,4}$, so the attachment yields $\Sigma_{g+1,3}$. Note now that C_1 or C_2 may meet only one boundary component of $\Sigma_{g+1,3}$.

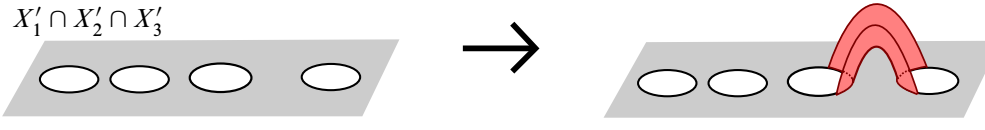

Figure 13: The boundary-stabilization move adds a band $I \times (B_1 \cap B_2 \cap B_+)$ to the triple intersection $X_1' \cap X_2' \cap X_3'$.

$\boldsymbol{X_1' \cap \partial}$ Before boundary-stabilizing X_3', we have $X_1' \cap \partial \cong S^1 \times B^2$. After boundary-stabilizing X_3', $X_1' \cap \partial \cong S^1 \times B^2$. From $X_1' \cap \partial$, in the boundary-stabilization we carve out a neighborhood of arc C in $\partial(X_1' \cap \partial)$. This does not change the topology of $X_1' \cap \partial$.

$\boldsymbol{X_2' \cap \partial}$ Before boundary-stabilizing X_3', we have $X_2' \cap \partial \cong S^1 \times B^2$. After boundary-stabilizing X_3', $X_2' \cap \partial \cong S^1 \times B^2$. From $X_2' \cap \partial$, in the boundary-stabilization we carve out a neighborhood of arc C in $\partial(X_2' \cap \partial)$. This does not change the topology of $X_2' \cap \partial$.

$\boldsymbol{X_3' \cap \partial}$ Before boundary-stabilizing X_3', we have $X_3' \cap \partial \cong S^1 \times B^2$. After boundary-stabilizing X_3', $X_3' \cap \partial \cong \natural_2 S^1 \times B^2$. To $X_3' \cap \partial$, we add $\nu(C) \cap \partial =$ (arc parallel to C) $\times D^2$ (recall $C \subset X_1' \cap X_2' \cap \partial X$). The effect is to add another boundary-sum $S^1 \times B^2$ component to $X_3' \cap \partial$.

$\boldsymbol{X_1' \cap X_2' \cap \partial}$ Before boundary-stabilizing X_3', $X_1' \cap X_2' \cap \partial \cong \bigsqcup_2 S^1 \times I =$ (two annuli). After boundary-stabilizing X_3', $X_1' \cap X_2' \cap \partial \cong D^2 \sqcup (S^1 \times I)$. From $X_1' \cap X_2' \cap \partial$, in the boundary-stabilization we carve out a neighborhood of arc C, which is a cocore of one annulus.

$\boldsymbol{X_2' \cap X_3' \cap \partial}$ Before boundary-stabilizing X_3', $X_2' \cap X_3' \cap \partial \cong \bigsqcup_2 S^1 \times I =$ (two annuli). After boundary-stabilizing X_3', $X_2' \cap X_3' \cap \partial \cong \left(\bigsqcup_2 S^1 \times I\right) \cup$ (band) $\cong \Sigma_{0,3}$. To $X_2' \cap X_3' \cap \partial$, we add $I \times (B_2 \cap D_+ \cap D_-)$.

$\boldsymbol{X_1' \cap X_3' \cap \partial}$ Before boundary-stabilizing X_3', $X_1' \cap X_3' \cap \partial \cong \bigsqcup_2 S^1 \times I =$ (two annuli). After boundary-stabilizing X_3', $X_1' \cap X_3' \cap \partial \cong \left(\bigsqcup_2 S^1 \times I\right) \cup$ (band) $\cong \Sigma_{0,3}$. To $X_1' \cap X_3' \cap \partial$, we add $I \times (B_1 \cap D_+ \cap D_-)$.

$\boldsymbol{X_1' \cap X_2' \cap X_3' \cap \partial}$ Before boundary-stabilizing X_3', $X_1' \cap X_2' \cap X_3' \cap \partial \cong \bigsqcup_4 S^1$, the boundary components of $X_1' \cap X_2' \cap X_3'$. After boundary-stabilizing X_3', we have $X_1' \cap X_2' \cap X_3' \cap \partial \cong \bigsqcup_3 S^1$. During the boundary-stabilization, we surger $X_1' \cap X_2' \cap X_3' \cap \partial$ along the two intervals in $\nu(C)$. The band we surger along is $I \times (B_1 \cap B_2 \cap D_-)$; we delete neighborhoods of $\partial I \times (B_1 \cap B_2 \cap D_-)$ and glue in the remaining boundary. We assumed that the endpoints of C met different boundary components of $X_1' \cap X_2' \cap X_3'$, which causes the number of components of $X_1' \cap X_2' \cap X_3' \cap \partial$ to decrease after the boundary-stabilization. If we did the same procedure on an arc with both endpoints on one boundary component then after the boundary-stabilization we would have had $X_1' \cap X_2' \cap X_3' \cap \partial = \bigsqcup_5 S^1$. This concludes the analysis of the effect of boundary-stabilizing X_3' along $C = C_3$.

Now similarly boundary-stabilize X_1' along C_1 and X_2' along C_2 to obtain $X^4\setminus\nu(S)=\widetilde{X}_1\cup\widetilde{X}_2\cup\widetilde{X}_3$ (where $\widetilde{X}_i$ is obtained from X_i' by performing all three boundary stabilizations). The end result will have $\widetilde{X}_i\cap\widetilde{X}_j\cap\partial(X^4\setminus\nu(S))=$ (thrice-punctured sphere) or (once-punctured torus), depending on our choice of arcs C_1, C_2 and C_3 (see Figure 14).

One point of these boundary-stabilizations is to ensure that $\widetilde{X}_i\cap\widetilde{X}_j\cap\partial(X^4\setminus\nu(S))$ is connected. We must furthermore check that $\widetilde{X}_i\cap\partial(X^4\setminus\nu(S))$ is a product $\big(\widetilde{X}_i\cap\widetilde{X}_j\cap\partial(X^4\setminus\nu(S))\big)\times I$ and also a product $\big(\widetilde{X}_i\cap\widetilde{X}_k\cap\partial(X^4\setminus\nu(S))\big)\times I$ (and that these two product structures agree), so that there is an induced open book on the boundary of $X^4\setminus\nu(S)$.

Claim 4.2 *$\widetilde{X}_1\cap\partial(X^4\setminus\nu(S))$ is a product over $\widetilde{X}_1\cap\widetilde{X}_2\cap\partial(X^4\setminus\nu(S))$ and over $\widetilde{X}_1\cap\widetilde{X}_3\cap\partial(X^4\setminus\nu(S))$. Moreover, these product structures agree.*

Proof See Figure 14 for an illustration of this proof.

Before any boundary-stabilizations, $X_1'\cap\partial$ is a solid torus. $X_1'\cap X_2'\cap\partial$ and $X_1'\cap X_3'\cap\partial$ are each disjoint unions of two annuli. The core of each annulus is a longitude of the solid torus $X_1'\cap\partial$.

From the discussion so far in this section, recall that after performing the X_3'–boundary stabilization we have

$$\begin{aligned} X_1'\cap\partial &\cong S^1\times B^2,\\ X_1'\cap X_2'\cap\partial &\cong D^2\sqcup(S^1\times I),\\ X_1'\cap X_3'\cap\partial &\cong \bigsqcup_2(S^1\times I)\cup(\text{band between the two components})\cong\Sigma_{0,3}. \end{aligned}$$

Similarly, after further performing the X_2'–boundary stabilization we have

$$\begin{aligned} X_1'\cap\partial &\cong S^1\times B^2,\\ X_1'\cap X_2'\cap\partial &\cong D^2\sqcup(S^1\times I)\cup(\text{band between the two components})\cong S^1\times I,\\ X_1'\cap X_3'\cap\partial &\cong \Sigma_{0,3}\setminus\nu(\text{arc between two boundary components})\cong S^1\times I. \end{aligned}$$

Thus, after performing the X_2' and X_3' boundary-stabilizations, $X_1'\cap\partial$ is a solid torus and each of $X_1'\cap X_2'\cap\partial$ and $X_1'\cap X_3'\cap\partial$ is an annulus on $\partial(X_1'\cap\partial)$ whose core is a longitude of $X_1'\cap\partial$. At this point, we have a product structure $X_1'\cap\partial\cong(S^1\times I\times I)$, where $X_1'\cap X_2'\cap\partial=S^1\times I\times 0$ and $X_1'\cap X_3'\cap\partial=S^1\times I\times 1$.

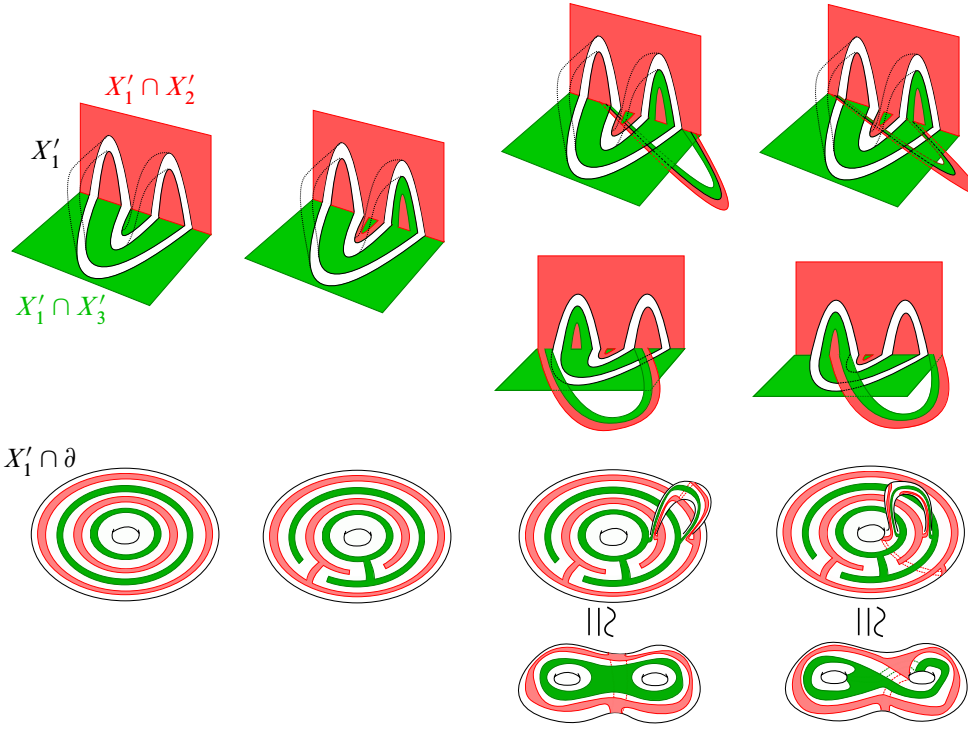

Figure 14: Top left: a schematic of X_1'. To the right, we draw X_1' after boundary-stabilizing X_2' and X_3'. Top two, third column: two perspectives of $\widetilde{X}_1$ after boundary-stabilizing X_1'. Top two, rightmost: two perspectives of $\widetilde{X}_1$ after a boundary-stabilizing X_1' (with a different choice of C_1). Bottom left: before boundary-stabilizing, $X_1' \cap \partial$ is a solid torus. On its boundary, $X_1' \cap X_2' \cap \partial$ and $X_1' \cap X_3' \cap \partial$ are each two longitudinal annuli. Bottom left, second picture: $X_1' \cap \partial$ after boundary-stabilizing X_2' and X_3'. Bottom left, two rightmost pictures: $\widetilde{X}_1 \cap \partial$ after boundary-stabilizing X_1' for two different choices of C_1 (corresponding to the images in the top row).

The X_1' boundary-stabilization increases the genus of $X_1' \cap \partial$. On the solid tube added to $X_1' \cap \partial$ to obtain $\widetilde{X}_1 \cap \partial$, there is a band on the boundary (parallel to the core of the tube) contained in $\widetilde{X}_1 \cap \widetilde{X}_2 \cap \partial$ and another band on the boundary (parallel to the core of the tube) contained in $\widetilde{X}_1 \cap \widetilde{X}_3 \cap \partial$. The effect on the product structure of $X_1' \cap \partial$ is to add a product tube (band) $\times I$. □

The above claim holds similarly for $\widetilde{X}_2 \cap \partial$ and $\widetilde{X}_3 \cap \partial$, exchanging the roles of $\widetilde{X}_1$, $\widetilde{X}_2$ and $\widetilde{X}_3$. Thus, $(\widetilde{X}_1, \widetilde{X}_2, \widetilde{X}_3)$ induces an open-book structure on $\partial(X^4 \setminus \nu(S))$, so $(\widetilde{X}_1, \widetilde{X}_2, \widetilde{X}_3)$ is a relative trisection of $X^4 \setminus \nu(S)$.

In conclusion, we now show how to find a relative trisection diagram $(\Sigma', \alpha', \beta', \gamma')$ of this relative trisection. See Figure 15 for several simple examples. We start with a shadow diagram $(\Sigma, \alpha, \beta, \gamma, s_\alpha, s_\beta, s_\gamma)$ of S (recall Definition 2.4). Stabilize $(\Sigma, \alpha, \beta, \gamma)$ as necessary so that we may take s_α, s_β and s_γ each to be two disjoint arcs. Identify Σ with $X_1 \cap X_2 \cap X_3$. The arcs C_1, C_2 and C_3 are parallel to one arc of s_β, s_γ and s_α, respectively (with correct framing, since we assumed that C_k does not twist around $S \cap X_i \cap X_j$ in $X_i \cap X_j$).

Obtain Σ' from Σ by first deleting an open neighborhood of ∂s_* and then attaching an orientation-preserving band for each C_i (with endpoints around ∂C_i). The core of C_3 and its shadow (an arc in s_α) together bound a disk in $\widetilde{X}_1 \cap \widetilde{X}_2$, giving an α' curve (shadow of C_3) $\cup$ (core of band corresponding to C_3). The other α' curve encircles the shadow of C_3 in Σ. Similar holds for the β' and γ' curves. See Figure 15 for several small examples of relatively trisecting $X^4 \setminus \nu(S)$.

To obtain a relative trisection of $X^4 \setminus \nu(S)$ with $p = 0$ and $b = 3$ (which will be desired in Section 5), we fix one intersection of $X_1 \cap X_2 \cap X_3 \cap S$ and choose the boundary-stabilizations to never meet the corresponding boundary component of $X_1' \cap X_2' \cap X_3'$. This ensures that the resulting triple-intersection of the relative trisection on $X^4 \setminus \nu(S)$ has three boundary components.

4.2 Trisecting complements of arbitrary surfaces

In this section, we trisect the complement of an arbitrary surface S in X^4. The construction is similar to $\mathbb{R}P^2$ case. Many indices are included for the very-interested reader. Averagely interested readers may ignore these numbers.

Let $S \subset X^4$ be a connected surface with $\chi(S) = \chi$, in a (g, k)–trisected 4–manifold $X^4 = (X_1, X_2, X_3)$. Isotope S so that (X_1, X_2, X_3) induces a $(c, b) = \left(\frac{1}{3}(\chi+b), b\right)$–trisection of S. By [18], we can stabilize each X_i $\frac{1}{3}(\chi+b-1)$ times so that $\frac{1}{3}(\chi+b) = c = 1$ and $b = 3-\chi$ (this increases g and k). Delete a tubular neighborhood of S; let $X_i' := X_i \setminus \nu(S)$.

As in Section 4.1, take C_1, C_2 and C_3 to be collections of $2-\chi$ disjoint arcs with endpoints on $X_1' \cap X_2' \cap X_3'$, with $C_i \subset X_j' \cap X_k' \cap \partial$. Take each arc in C_i to be parallel to a distinct arc in $\nu(S) \cap X_j \cap X_k$; there is exactly one arc in $S \cap X_j \cap X_k$ which is not parallel to any arc in C_i. Moreover, take each arc of C_i to twist zero times around the 3–dimensional tubes of $\nu(S) \cap (X_j \cap X_k)$ (ie we ask that $S \cap (X_j \cap X_k)$ cobounds

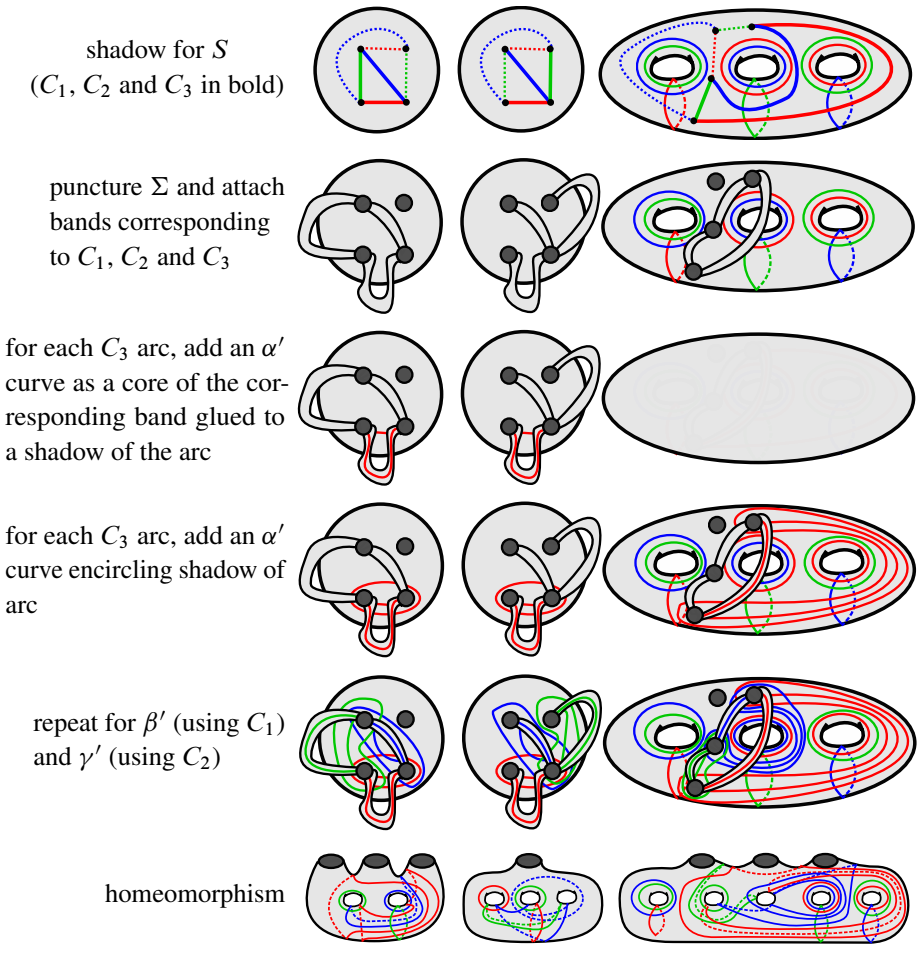

Figure 15: Illustration of the process for finding a relative trisection of $X^4 \setminus \nu(S)$, where $S \cong \mathbb{R}P^2$. In the top row, we draw possible shadow diagrams for S. Down each column, we show the process in finding the relative trisection, where the bold shadows are parallel to the chosen arcs C_1, C_2 and C_3. The final relative trisection is in the 5^{th} row; we give an equivalent diagram (related by a surface automorphism) in the 6^{th} row. Left to right, the final relative trisections have (g, k, p, b) respectively equal to $(2, 2, 0, 3)$, $(3, 2, 1, 1)$ and $(5, 3, 0, 3)$.

disks D in $X_j \cap X_k$ with arcs in $X_i \cap X_j \cap X_k$, so that $C_i \cap D = \varnothing$). Finally, take C_1, C_2 and C_3 to have disjoint endpoints.

Let $(\widetilde{X}_1, \widetilde{X}_2, \widetilde{X}_3)$ be the result of boundary-stabilizing (X_1', X_2', X_3') along every arc in $C_1 \cup C_2 \cup C_3$ (ie boundary-stabilizing X_1' along C_1, X_2' along C_2 and X_3' along C_3).

Proposition 4.3 $(\widetilde{X}_1, \widetilde{X}_2, \widetilde{X}_3)$ *is a relative trisection of* $X^4 \setminus \nu(S)$.

Proof Recall X_i' is a 4–dimensional handlebody, and $\widetilde{X}_i$ is obtained from X_i' by attaching 1–handles. Therefore, $\widetilde{X}_i$ is a 4–dimensional handlebody. In fact, $\widetilde{X}_i = X_i' \natural_{(2-\chi)}(S^1 \times B^3) \cong \natural_{k+3-\chi} S^1 \times B^3$.
Moreover, $\widetilde{X}_i \cap \widetilde{X}_j$ is formed by attaching 3–dimensional 1–handles to the 3–dimensional handlebody $X_i' \cap X_j'$, so $\widetilde{X}_i \cap \widetilde{X}_j$ is a 3–dimensional handlebody. In fact, $\widetilde{X}_i \cap \widetilde{X}_j = (X_i' \cap X_j') \natural \natural_{2(2-\chi)}(S^1 \times D^2) \cong \natural_{g+7-3\chi} S^1 \times D^2$.
Furthermore, the triple intersection $\widetilde{X}_1 \cap \widetilde{X}_2 \cap \widetilde{X}_3$ is formed from $X_1' \cap X_2' \cap X_3'$ by attaching $3(2-\chi)$ orientation-preserving bands. Therefore, $\widetilde{X}_1 \cap \widetilde{X}_2 \cap \widetilde{X}_3$ is a connected, orientable surface of Euler characteristic $2-2g-2(3-\chi)-3(2-\chi) = -10-2g+5\chi$. The genus and number of boundary components of this triple intersection depends on the choice of C_1, C_2 and C_3. To finish the proof, we need to show that the proposed relative trisection induces an open book decomposition on the boundary.

Claim 4.4 $\widetilde{X}_1 \cap \partial(X^4 \setminus \nu(S))$ *is a product over* $\widetilde{X}_1 \cap \widetilde{X}_2 \cap \partial(\widetilde{X}^4 \setminus \nu(S))$ *and over* $\widetilde{X}_1 \cap \widetilde{X}_3 \cap \partial(\widetilde{X}^4 \setminus \nu(S))$. *Moreover, these product structures agree.*

Proof The proof is virtually the same as in Section 4.1; see Figure 14.

Note $X_1' \cap X_2' \cap \partial(X^4 \setminus \nu(S))$ consists of $3-\chi$ longitudinal annuli on the solid torus $X_1' \cap \partial(X^4 \setminus \nu(S))$. After boundary-stabilizing X_3' a total of $2-\chi$ times along C_3,

$$\begin{aligned} X_1' \cap \partial &\cong S^1 \times B^2, \\ X_1' \cap X_2' \cap \partial &\cong \bigsqcup_{2-\chi} D^2 \sqcup (S^1 \times I), \\ X_1' \cap X_3' \cap \partial &\cong \bigsqcup_{3-\chi} (S^1 \times I) \cup (2-\chi \text{ bands}) \cong \Sigma_{0,4-\chi}. \end{aligned}$$

In the above, we implicitly use the fact that the intersection of S with X_1 is a single disk. This ensures that attaching bands to $X_1' \cap X_3' \cap \partial$ parallel to arcs C_3 in $X_1' \cap X_2' \cap \partial$ does not increase the genus of $X_1' \cap X_3' \cap \partial$, as each successive band must join two distinct components.

After further boundary-stabilizing X_2' $2-\chi$ times along C_2, we have

$$\begin{aligned} X_1' \cap \partial &\cong S^1 \times B^2, \\ X_1' \cap X_2' \cap \partial &\cong \bigsqcup_{2-\chi} D^2 \sqcup (S^1 \times I) \cup (2-\chi \text{ bands}) \cong S^1 \times I, \\ X_1' \cap X_3' \cap \partial &\cong \Sigma_{0,4-\chi} \setminus \nu(2-\chi \text{ arcs}) \cong S^1 \times I. \end{aligned}$$

In the above, we implicitly use the fact that the intersection of S with X_1 is a single disk. This ensures that attaching bands to $X_1' \cap X_2' \cap \partial$ parallel to arcs C_2 in $X_1' \cap X_3' \cap \partial$ does not increase the genus of $X_1' \cap X_2' \cap \partial$, as each successive band must join two distinct components. We also use the fact that the arcs C_2 meet $2(2-\chi)-2$ distinct boundary components of $X_1' \cap X_2' \cap X_3'$. Each successive deletion from $X_1' \cap X_3' \cap \partial$ must decrease the number of boundary components.

Thus, after performing the X_2' and X_3' boundary-stabilizations, $X_1' \cap \partial$ is a solid torus and each of $X_1' \cap X_2' \cap \partial$ and $X_1' \cap X_3' \cap \partial$ is an annulus on $\partial(X_1' \cap \partial)$ whose core is a longitude of $X_1' \cap \partial$. At this point, we have a product structure $X_1' \cap \partial \cong (S^1 \times I \times I)$, where $X_1' \cap X_2' \cap \partial = S^1 \times I \times 0$ and $X_1' \cap X_3' \cap \partial = S^1 \times I \times 1$.

The X_1' boundary-stabilizations along C_1 increases the genus of $X_1' \cap \partial$ by $2-\chi$, yielding $\widetilde{X}_1 \cap \partial \cong \natural_{3-\chi} S^1 \times D^2$. On each of the $2-\chi$ solid tubes added to X_1' to form $\widetilde{X}_1$, there is a band on the boundary (parallel to the core of the tube) contained in $\widetilde{X}_1 \cap \widetilde{X}_2 \cap \partial$ and another band on the boundary (parallel to the core of the tube) contained in $\widetilde{X}_1 \cap \widetilde{X}_3 \cap \partial$. The effect on the product structure of $X_1' \cap \partial$ is to add $2-\chi$ product tubes of the form (band) $\times I$. □

The above claim holds similarly for $\widetilde{X}_2 \cap \partial$ and $\widetilde{X}_3 \cap \partial$, interchanging the roles of $\widetilde{X}_1, \widetilde{X}_2$ and $\widetilde{X}_3$. Thus, $(\widetilde{X}_1, \widetilde{X}_2, \widetilde{X}_3)$ is a relative trisection for $X^4 \setminus \nu(S)$. □

Now we will explicitly trisect the complement of a specific surface S. We start from a shadow diagram $(\Sigma, \alpha, \beta, \gamma, s_\alpha, s_\beta, s_\gamma)$ for S. We stabilize X_1, X_2 and X_3 until each of s_α, s_β and s_γ consists of $3-\chi$ arcs, as in [18]. Identify Σ with $X_1 \cap X_2 \cap X_3$. Now choose $2-\chi$ distinct components of s_α, s_β and s_γ (each) to be (parallel to) C_3, C_1 and C_2, respectively. We obtain a relative trisection diagram $(\Sigma', \alpha', \beta', \gamma')$ for $(\widetilde{X}_1, \widetilde{X}_2, \widetilde{X}_3)$ by doing the following:

- Delete open neighborhoods of the endpoints of s_* from Σ. Attach an orientation-preserving band for each component of C_1, C_2 and C_3, with endpoints of the band around endpoints of the arc component. Call the resulting surface Σ'.
- Take $\alpha \subset \alpha'$, $\beta \subset \beta'$ and $\gamma \subset \gamma'$.
- For each arc in C_3, obtain an α' curve

  $$(\text{shadow of } C_3) \cup (\text{core of band corresponding to } C_3).$$

  Similarly obtain a β' and γ' curve for each component of C_1 and C_2, respectively.

- For each arc in C_3, obtain an α' curve which encircles the shadow of C_3. Similarly obtain β' and γ' curves by encircling the shadows of C_1 and C_2, respectively.

This yields $g+4-2\chi(S)$ linearly independent α' curves on Σ'. As in Section 4.1, each α' curve bounds a disk in $\widetilde{X}_1 \cap \widetilde{X}_2$. Moreover, we note

$$\chi(\Sigma') = 2-2g-2(3\chi)-3(2-\chi) = -10-2g+5\chi,$$

so $\chi(\Sigma' \times I) \cong \partial_{11+2g-5\chi}(S^1 \times B^3)$. Recall

$$\widetilde{X}_1 \cap \widetilde{X}_2 \cong \natural_{g+(3-\chi(S))+2(2-\chi(S))} (S^1 \times B^2) \cong \natural_{g+7-3\chi(S)} (S^1 \times B^2).$$

Therefore, in a relative trisection diagram for $(\widetilde{X}_1, \widetilde{X}_2, \widetilde{X}_3)$ there are $g+4-2\chi$ distinct α' curves altogether. Thus, we have listed the complete set of α' curves (and similarly β' and γ' curves).

In Figure 16, we consider $S =$ (spun trefoil) # (unknotted torus) $\subset S^4$ (a triplane diagram can be obtained by connect-summing diagrams from [17]; we convert this into a shadow diagram). The torus S can be isotoped so that the standard $(0,0)$–trisection (X_1, X_2, X_3) of S^4 induces a $(2,6)$–bridge trisection of S. We stabilize each X_i once along an arc in $X_j \cap X_k \cap S$ to find a $(3,1)$–trisection of S^4 inducing a $(1,3)$–bridge trisection of S; the shadow diagram $(\Sigma, \alpha, \beta, \gamma, s_\alpha, s_\beta, s_\gamma)$ of Figure 16 illustrates this bridge trisection. To obtain a relative trisection of $S^4 \setminus \nu(S)$, we choose two arcs in each $X_j \cap X_k \cap S$ be parallel to $C_i \subset \partial\nu(S^4 \setminus \nu(S))$. In Figure 16, we indicate shadows of C_i in s_*. We then delete $\nu(S)$ and boundary stabilize each $X_i' := X_i \setminus \nu(S)$ (twice) along C_i to obtain a relative trisection $(\widetilde{X}_1, \widetilde{X}_2, \widetilde{X}_3)$ of $S^4 \setminus \nu(S)$.

To obtain the relative trisection diagram $(\Sigma', \alpha', \beta', \gamma')$ of $(\widetilde{X}_1, \widetilde{X}_2, \widetilde{X}_3)$ pictured in Figure 16 (bottom), we remove open neighborhoods of ∂s_* from Σ and attach six bands with ends at the boundary of C_1, C_2 and C_3. Then we include two α' curves for each arc in C_3: one curve is the shadow of C_3 plus a core of the corresponding band, while one curve encircles the shadow of the arc in C_3. We similarly add four β' and γ' curves (each) corresponding to C_1 and C_2, respectively. In recap, there are seven total α' curves, given by:

- The α curves in the trisection (X_1, X_2, X_3) of S^4. In this example, (X_1, X_2, X_3) is a $(3,1)$–stabilization, so there are three such α' curves.

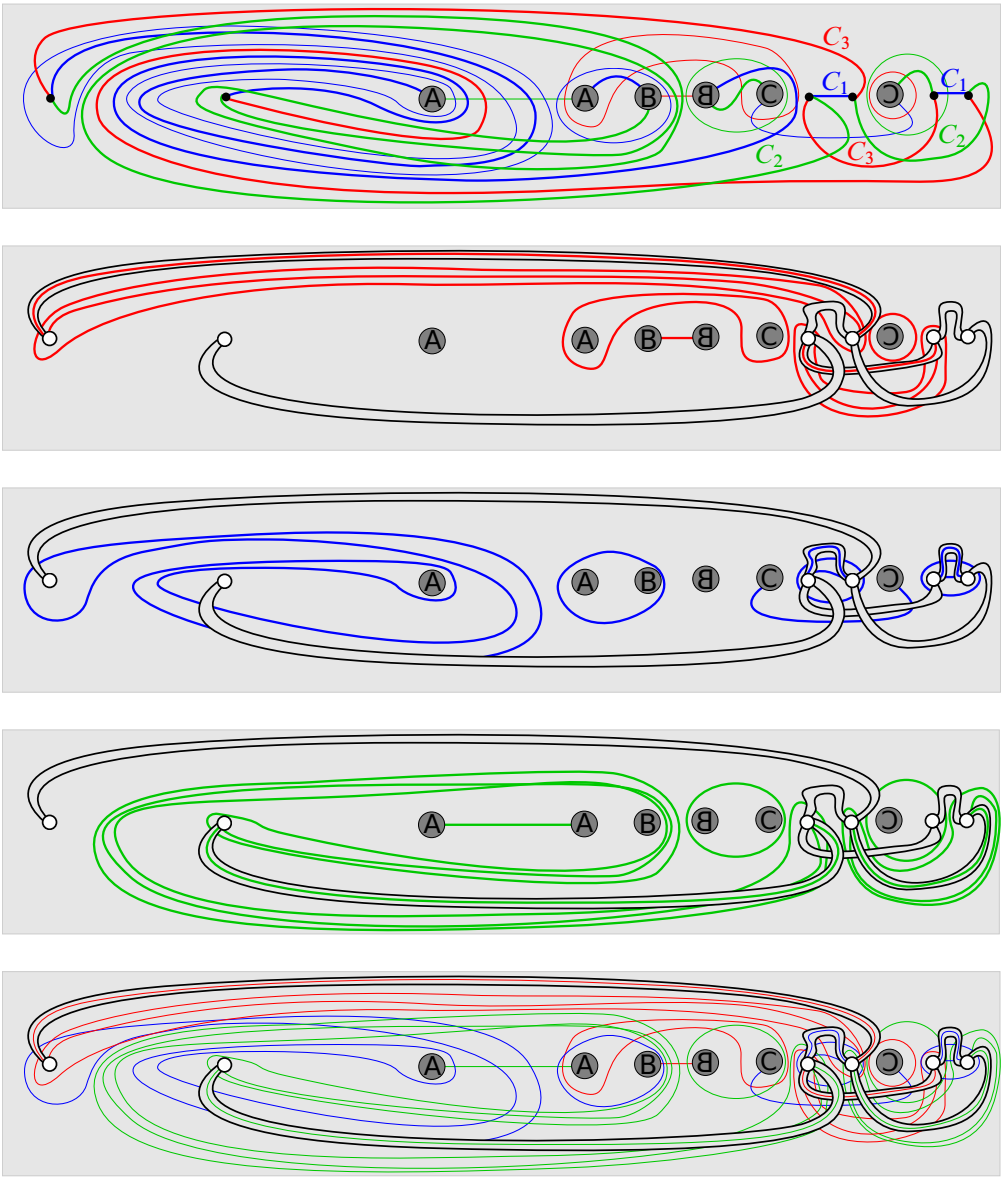

Figure 16: Top: a shadow diagram for a $S = (\text{spun trefoil}) \# (\text{unknotted torus})$ in S^4. Note S is in $(1,3)$–bridge position. We indicate two arcs in each s_* that comprise C_1, C_2, and C_3 in the construction of a relative trisection of $S^4 \setminus \nu(S)$. We will obtain a diagram $(\Sigma', \alpha', \beta', \gamma')$ of this relative trisection. Second row: Σ' and α'. Third row: Σ' and β'. Fourth row: Σ' and γ'. Bottom: the relative trisection $(\Sigma', \alpha', \beta', \gamma')$. This relative trisection of $S^4 \setminus \nu(S)$ has $(g, k, p, b) = (8, 4, 1, 2)$.

- Curves $a \cup a'$, where a is a shadow of an arc in C_3 and a' is a core of the band corresponding to that component of C_3. There are two such α' curves in this example.
- Curves encircling the shadows of C_3. In this example there are two such α' curves.

The seven β' and γ' curves are similarly related to β and C_1, and γ and C_2, respectively.

5 Gluing $P_\pm$ to $X^4 \setminus \mathbb{R}P^2$

Let $S \subset X^4$ be an $\mathbb{R}P^2$ with Euler number $e(S) = \pm 2$. We have previously produced preferred $(g, k, p, b) = (2, 2, 0, 3)$–trisections T_1 and T_2 (or $\overline{T}_1$ and $\overline{T}_2$ if $e(S) = -2$) of $\nu(S)$ (see Section 3.2), and can produce a $(g, k, 0, 3)$–trisection of $X^4 \setminus \nu(S)$ via Section 4.1. The following easy lemma allows us to glue these trisections:

Lemma 5.1 *Suppose Q has an open book where the pages are 3–punctured spheres. Then the monodromy of the open book consists of two Dehn twists around each boundary, not all of the same sign.*

Proof Suppose the monodromy of the open book consists of a, b and c Dehn twists about the three boundary components correspondingly for $a, b, c \in \mathbb{Z}$. Then Q is a Seifert fibered space over S^2 with three exceptional fibers of orders a, b and c. Then $\pi_1(Q) = \langle x_1, x_2, x_3, h \mid [x_i, h] = x_1^a h = x_2^b h = x_3^c h = x_1 x_2 x_3 = 1 \rangle$. But recall also that $\pi_1(Q)$ is the quaternion group. Then $h \in Z(\pi_1(Q))$ implies $h = \pm 1$.

We have $\mathbb{Z}/2 \oplus \mathbb{Z}/2 = H_1(Q)$ is the abelianization of $\pi_1(Q)$. So, if $h = 1$, $\mathbb{Z}/2 \oplus \mathbb{Z}/2 \cong \langle x_1, x_2 \mid a x_1 = b x_2 = c(x_1 + x_2) = 0 \rangle$. This implies a and b are even, but neither x_1 nor x_2 can be ± 1 (or else $H_1(Q)$ would be cyclic). Therefore, $4 \mid (a, b, c)$, giving abelianization $\mathbb{Z}/4 \oplus \mathbb{Z}/4$, a contradiction. Thus, $h = -1$.

Now $h = -1$, and

$$\mathbb{Z}/2 \oplus \mathbb{Z}/2 = \pi_1(Q)/\langle -1 \rangle = \langle x_1, x_2, x_3 \mid x_1^a = x_2^b = x_3^c = x_1 x_2 x_3 = 1 \rangle.$$

By multiplying the x_i by -1 and/or replacing x_i with x_i^{-1}, we see this group is isomorphic to the triangle group $\langle x, y, z \mid x^{|a|} = y^{|b|} = z^{|c|} = xyz = 1 \rangle$. Since $\pi_1(Q)/\langle -1 \rangle = \mathbb{Z}/2 \oplus \mathbb{Z}/2$ is finite and dihedral, this is a spherical triangle group with $|a| = |b| = |c| = 2$. Computing $4 = |H_1(Q)| = |ab + bc + ca|$ yields $\{a, b, c\} = \pm\{2, 2, -2\}$. □

Corollary 5.2 *Let T be a $(g,k,0,3)$–trisection of $X^4 \setminus \nu(S)$ produced by the algorithm of Section 4.1. If $e(S)=2$, then the monodromy on the open book induced by T has left-handed twists about two bindings and right-handed twists about the other (mirrored for $e(S)=-2$).*

Proof Say $e(S)=2$. Fix $Q=\partial P_+$ with singular fibers S_0, S_1 and S_{-1}. We saw in Section 3.2 that T_1 and T_2 each have monodromy consisting of right-handed twists about two boundaries and left-handed twists about the other. Suppose the same is true for T. If the left-handed boundary corresponds to S_{-1}, then we see T_1 and T induce the same orientation on Q. Similarly, if the left-handed boundary corresponds to S_0 or S_1, then we see T induces the same orientation on Q as T_2. In either case, we find $X^4 \setminus P_+$ and P_+ induce the same orientation on Q, a contradiction. □

Corollary 5.3 *Let T be a $(g,k,0,3)$–trisection of $X^4 \setminus \nu(S)$. Say $e(S)=2$. We may glue T to T_1 or T_2 to obtain $(g+4,k)$–trisections of X^4, $\tau_S(X^4)$ and $\Sigma_S(X^4)$.* (If $e(S)=-2$, then the result holds for gluing T to $\overline{T}_1$ or $\overline{T}_2$.)

Proof By Corollary 5.2, $\overline{T}$, T_1 and T_2 induce homeomorphic open books on Q. By gluing T and T_1, we may identify $S_{-1} \subset Q = \partial P_+$ with the right-hand twist boundary of T. By gluing T and T_2, we may identify S_{-1} with either of the left-hand twist boundaries of T. Thus, we produce trisections of three 4–manifolds $\nu(S) \cup_\phi (X^4 \setminus \nu(S))$, where $\phi\colon Q \to Q$ preserves the Seifert fiber structure and can be chosen to map S_{-1} to any singular fiber. By the discussion in Section 3.1, these manifolds are X^4, $\tau_S(X^4)$ and $\Sigma_S(X^4)$.

To see that the result of gluing T and T_i is a $(g+4,k)$–trisection, recall that T_i is a $(g',k',p,b)=(2,2,0,3)$–relative trisection. Then the result of gluing T to T_i is a $(g+g'+(b-1), k+k'-(2p+b-1))=(g+4,k)$–trisection. □

5.1 Example

Finally, we present an example of trisecting the result of $\mathbb{R}P^2$ surgery. Let $S \cong \mathbb{R}P^2 \subset S^4$ be the connect-sum of the spun trefoil and an unknotted $\mathbb{R}P^2$ with Euler number -2. We first isotope S to be in $(c,b)=(1,2)$–bridge position with respect to a $(3,1)$–trisection of S^4. We depict a shadow diagram for S in Figure 17, top. This diagram can be obtained by understanding [17] (either the explicit example diagrams of twist-spun knots or the procedure to turn a movie of a knotted surface into a triplane diagram). We obtain a relative trisection $T=(\Sigma',\alpha',\beta',\gamma')$ of $S^4 \setminus \nu(S)$ as in

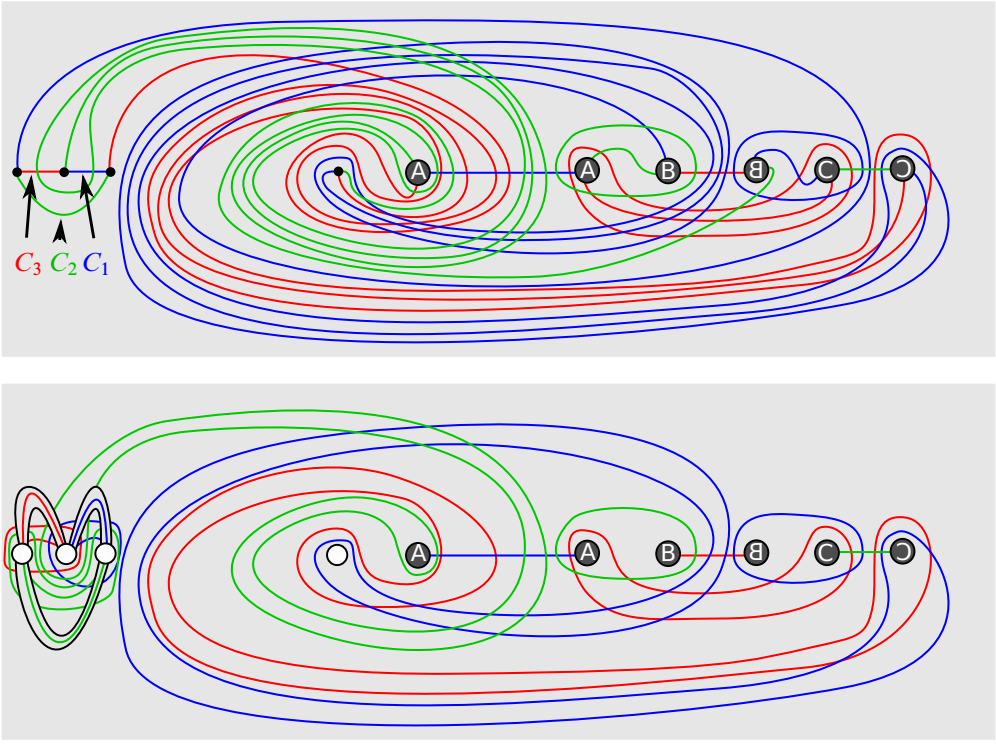

Figure 17: Top: A shadow diagram for S. Here, S is the connect-sum of the spun trefoil with an unknotted $\mathbb{R}P^2$ (Euler number -2) in S^4. We indicate shadows of arcs C_1, C_2 and C_3 to be used in finding a relative trisection T of $S^4 \setminus \nu(S)$. Bottom: A relative trisection diagram for T. Here, T has $(g, k, p, b) = (5, 3, 0, 3)$.

Section 4.1. A diagram of T is pictured in Figure 17, bottom, obtained as per the algorithm of Section 4.1. We specifically choose the arcs C_1, C_2 and C_3 so that Σ' has three boundary components.

To achieve surgery on S diagrammatically, we will glue T to $\overline{T}_1$ or $\overline{T}_2$ (our two preferred trisections of P_- from Section 3.2) as in Corollary 5.3. By Price [20] (see Section 3), the gluing of $S^4 \setminus \nu(S)$ and P_- is determined up to diffeomorphism by the identifications of $\partial\Sigma'$ with the boundary of the trisection surface of $\overline{T}_i$. In particular, the gluing is determined up to diffeomorphism by the choice of which boundary of Σ' is identified with the S_{-1} boundary component of $\overline{T}_i$. When gluing T to $\overline{T}_1$, the resulting manifold is therefore determined up to diffeomorphism. There are potentially two nondiffeomorphic choices resulting from gluings of T to $\overline{T}_2$.

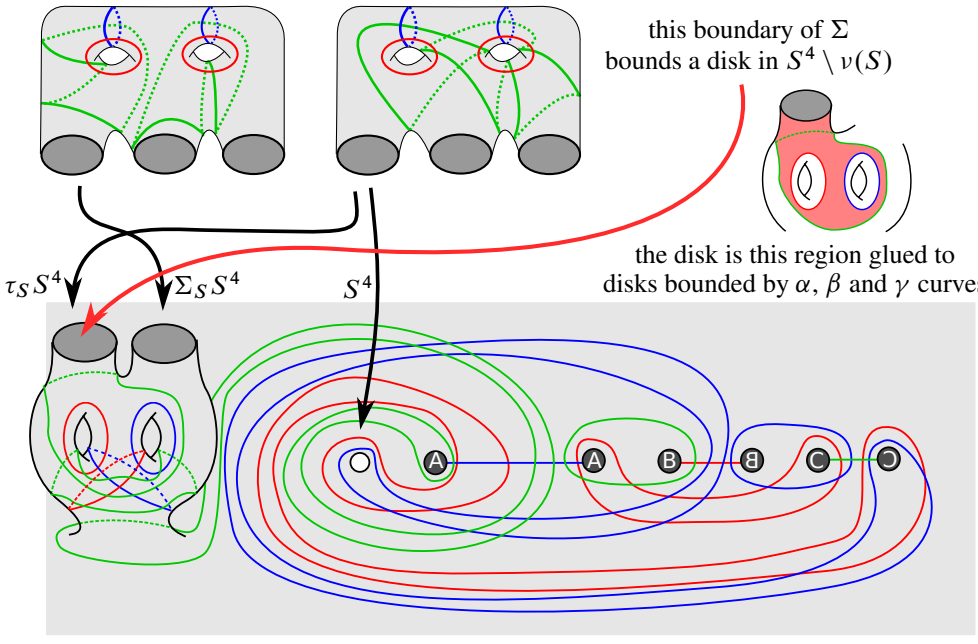

Figure 18: We obtain trisections of $S^4, \tau(S^4), \Sigma(S^4)$ by gluing $\overline{T}_1$ or $\overline{T}_2$ to T. The choice of which boundary of Σ' to identify with the S_{-1} boundary of the trisection surface of $\overline{T}_1$ or $\overline{T}_2$ determines the diffeomorphism type of the resulting trisected 4–manifold.

To glue T and $\overline{T}_i$, we must know the monodromy T induces on $\partial(S^4 \setminus \nu(S))$. We apply the monodromy algorithm of [6]. One need not perform the entire algorithm — the effect of the monodromy on one arc between the two leftmost boundary components of Σ' is to add two right-handed twists around the leftmost boundary components and two right-handed twists about the middle boundary component. By Corollary 5.2, the twists about the third boundary are right-handed.

The boundary of Σ' which does not meet any of the bands coming from boundary-stabilization (rightmost in Figure 18) corresponds to a meridian of S. Gluing the S_{-1} boundary of $\overline{T}_2$ to this boundary yields a trisection diagram of S^4.

Another (leftmost in Figure 18) boundary of Σ' corresponds to a curve in $\partial(S^4 \setminus \nu(S))$ which bounds a disk in $S^4 \setminus \nu(S)$. Gluing the S_{-1} singular fiber of ∂P_- to the corresponding singular fiber of $\partial(S^4 \setminus \nu(S))$ yields a manifold with nontrivial H_1; this is $\tau_S(S^4)$. Then gluing the S_{-1} boundary of $\overline{T}_1$ to this boundary of Σ' yields a trisection diagram of $\tau_S(S^4)$.

Gluing the S_{-1} boundary of $\overline{T}_2$ to the final boundary of Σ' (middle in Figure 18) yields a trisection diagram of $\Sigma_S(S^4)$.

We depict all the described gluings schematically in Figure 18. This relative trisection diagram of T agrees with the diagram of Figure 17 up to a surface automorphism and one handle-slide of the γ' curves.

6 Further questions

In Section 5.1, we know $\Sigma_S(S^4) \cong S^4$ because $S = K \# P_-$, where K is the spun trefoil. By [13], $\Sigma_S(S^4) \cong \Sigma_K(S^4) \cong S^4$.

Question 6.1 Using Gay and Meier's trisections of Gluck twists [10] and our trisections of Price twists, is there a trisection-theoretic proof of Katanaga, Saeki, Teragaito and Yamada's result [13]? That is, is there a trisection-theoretic proof that $\Sigma_K(X^4) \cong \Sigma_{K\#P_\pm}(X^4)$ for a 2–knot K with trivial Euler number? Possibly restricting to the case $X^4 = S^4$?

This question was recently answered affirmatively by P Naylor [19].

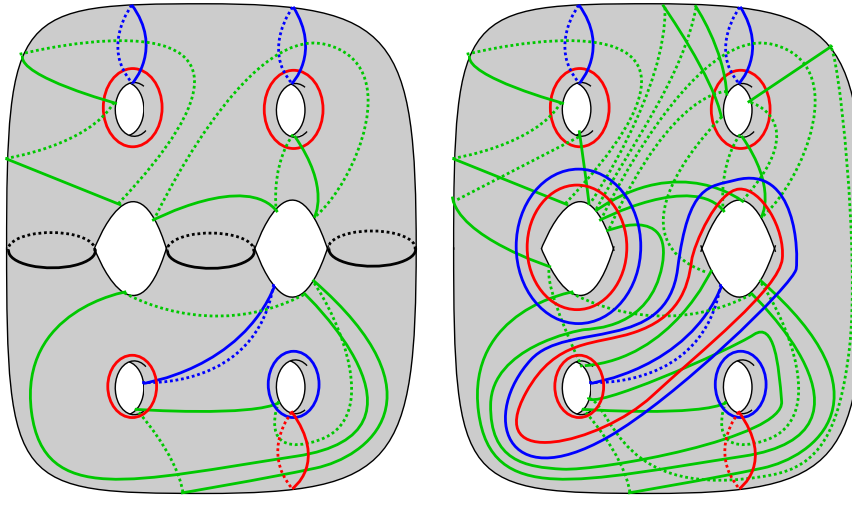

Figure 19: Left: We start to obtain a trisection T of $S^4 \cong \Sigma_{P_-}(S^4)$ by gluing $\overline{T}_1$ (top) to a relative trisection of $S^4 \setminus \nu(P_-)$ (bottom), obtained as in Section 5.1. This is not yet a trisection diagram, as the surface is genus-6 but there are only 4 (each) α, β, and γ curves. Right: We use the algorithm of [6] to find the two remaining α, β and γ curves (each) in T. Question 6.2 asks: is T a stabilization of the $(0,0)$–trisection of S^4?

When $\Sigma_S(S^4) \cong S^4$ we can ask about the complexity of the resulting trisection.

Question 6.2 Let S be a copy of $\mathbb{R}P^2$ embedded in S^4 so that $\Sigma_S(S^4) \cong S^4$. Let T be a trisection of $\Sigma_S(S^4) \cong S^4$ arising from the algorithm of Section 5. Is T a stabilized copy of the standard $(0,0)$–trisection on S^4?

This question is a specific case of a question/conjecture of [16].

Conjecture [16, Conjecture 3.11] Every trisection of S^4 is either the $(0,0)$–trisection or a stabilization of the $(0,0)$–trisection.

In Figure 19, we picture the simplest example of the trisections described in Question 6.2. This is a $(g,k)=(6,2)$–trisection of S^4 obtained by Price twisting $P_- \subset \mathbb{R}P^2$.

References

[1] **A Abrams**, **D T Gay**, **R Kirby**, *Group trisections and smooth 4–manifolds*, Geom. Topol. 22 (2018) 1537–1545 MR

[2] **S Akbulut**, *Constructing a fake 4–manifold by Gluck construction to a standard 4–manifold*, Topology 27 (1988) 239–243 MR

[3] **S Akbulut**, *Twisting 4–manifolds along $\mathbb{RP}^2$*, from "Proceedings of the Gökova Geometry–Topology Conference 2009" (S Akbulut, D Auroux, T Önder, editors), International, Somerville, MA (2010) 137–141 MR

[4] **S Akbulut**, **K Yasui**, *Corks, plugs and exotic structures*, J. Gökova Geom. Topol. 2 (2008) 40–82 MR

[5] **N A Castro**, *Relative trisections of smooth 4–manifolds with boundary*, PhD thesis, University of Georgia (2015) https://nickcastromath.files.wordpress.com/2015/11/thesis.pdf

[6] **N A Castro**, **D T Gay**, **J Pinzón-Caicedo**, *Diagrams for relative trisections*, Pacific J. Math. 294 (2018) 275–305 MR

[7] **N A Castro**, **D T Gay**, **J Pinzón-Caicedo**, *Trisections of 4–manifolds with boundary*, Proc. Natl. Acad. Sci. USA 115 (2018) 10861–10868 MR

[8] **N A Castro**, **B Ozbagci**, *Trisections of 4–manifolds via Lefschetz fibrations*, Math. Res. Lett. 26 (2019) 383–420 MR

[9] **D Gay**, **R Kirby**, *Trisecting 4–manifolds*, Geom. Topol. 20 (2016) 3097–3132 MR

[10] **D Gay**, **J Meier**, *Doubly pointed trisection diagrams and surgery on 2–knots*, preprint (2018) arXiv

[11] **S Kamada**, *Projective planes in 4–sphere obtained by deform-spinnings*, from "Knots 90" (A Kawauchi, editor), de Gruyter, Berlin (1992) 125–132 MR

[12] **S Kamada**, *A characterization of groups of closed orientable surfaces in 4–space*, Topology 33 (1994) 113–122 MR

[13] **A Katanaga**, **O Saeki**, **M Teragaito**, **Y Yamada**, *Gluck surgery along a 2–sphere in a 4–manifold is realized by surgery along a projective plane*, Michigan Math. J. 46 (1999) 555–571 MR

[14] **P Lambert-Cole**, *Bridge trisections in $\mathbb{CP}^2$ and the Thom conjecture*, preprint (2018) arXiv

[15] **F Laudenbach**, **V Poénaru**, *A note on 4–dimensional handlebodies*, Bull. Soc. Math. France 100 (1972) 337–344 MR

[16] **J Meier**, **T Schirmer**, **A Zupan**, *Classification of trisections and the generalized property R conjecture*, Proc. Amer. Math. Soc. 144 (2016) 4983–4997 MR

[17] **J Meier**, **A Zupan**, *Bridge trisections of knotted surfaces in S^4*, Trans. Amer. Math. Soc. 369 (2017) 7343–7386 MR

[18] **J Meier**, **A Zupan**, *Bridge trisections of knotted surfaces in 4–manifolds*, Proc. Natl. Acad. Sci. USA 115 (2018) 10880–10886 MR

[19] **P Naylor**, *Trisection diagrams and twists of 4–manifolds*, preprint (2019) arXiv

[20] **T M Price**, *Homeomorphisms of quaternion space and projective planes in four space*, J. Austral. Math. Soc. Ser. A 23 (1977) 112–128 MR

National Institute for Mathematical Sciences
Daejeon, South Korea

Current address: *Center for Geometry and Physics, Institute for Basic Science (IBS)*
Pohang, Republic of Korea

Department of Mathematics, Princeton University
Princeton, NJ, United States

math751@gmail.com, maggiem@math.princeton.edu

http://www.math.princeton.edu/~maggiem

Received: 19 September 2018 Revised: 15 February 2019